DALTON
FULL PAPER

Tetrathiafulvalene-functionalized phosphine as a coordinating ligand. X-Ray structures of $(PPh_2)_4TTF$ and $[(AuCl)_4\{(PPh_2)_4TTF\}]$

Elena Cerrada,[a] Carmelo Diaz,[b] M. Cristina Diaz,[b] Michael B. Hursthouse,[c] Mariano Laguna *[a] and Mark E. Light [c]

[a] *Departamento de Química Inorgánica, Instituto de Ciencia de Materiales de Aragón, Universidad de Zaragoza-C.S.I.C, E-50009 Zaragoza, Spain. E-mail: mlaguna@posta.unizar.es*
[b] *Escuela Superior de Huesca, Carretera de Zaragoza, s/n, 22071 Huesca, Spain*
[c] *Department of Chemistry, University of Southampton, Highfield, Southampton, UK SO17 1BJ*

Received 16th July 2001, Accepted 14th December 2001
First published as an Advance Article on the web 11th February 2002

The phosphine $(PPh_2)_4TTF$ (P4) (**1**) reacts with the gold(I) complexes [AuX(tht)] (X = Cl, C_6F_5; tht = tetrahydrothiophene) or [Au(Mes)($AsPh_3$)] (Mes = 2,4,6-$Me_3C_6H_2$) to give tetranuclear derivatives $[(AuX)_4P4]$ (X = Cl, **2**; C_6F_5, **3**; Mes, **4**). The analogous reaction starting with [Au(Trip)($AsPh_3$)] (Trip = 2,4,6-$Pr^i_3C_6H_2$) provides the dinuclear derivative $[(AuTrip)_2P4]$ (**5**). When the phosphine P4 reacts with $[Cu(MeCN)_4]PF_6$, $AgCF_3SO_3$ or $[Au(tht)_2]CF_3SO_3$ in a 2:1 molar ratio, complexes $[M(P4)_2]A$ (A = PF_6, M = Cu, **6**; A = CF_3SO_3, M = Ag, **7**, Au, **8**) are obtained, or $\{[M_2P4](CF_3SO_3)_2\}_n$ (M = Ag, **9**; Au, **10**) when 1:1 molar ratios are used instead. Visible-ultraviolet and electrochemical studies of the new complexes are reported. Two, reversible one-electron oxidations to the mono- and di-cation occur in complexes **2**–**10** at more positive potentials than the two reversible oxidations exhibited by the free P4 (**1**) ligand. The structures of **1** and **2** have been confirmed by X-ray analysis.

Introduction

During the past two decades there has been considerable interest in the synthesis of materials with tunable conducting, magnetic or optical properties. With reference to conduction, one of the prerequisites for high conductivity is a partially filled energy band. The stacking of planar (or near planar) π-donor or -acceptor molecules improves the overlap of the π-systems, developing the conduction band in this direction. In addition, an increase in the dimensionality of these materials, which for many systems has been achieved by interstack chalcogen–chalcogen interactions, is known to stabilize the metallic state by supressing the Peierls distorsion.[1] The introduction of heteroatoms such as S, Se and Te, with spatially extended p_π orbitals, increases the π-overlap and results in wider bands. Tetrathiafulvalene (TTF) and its derivatives[2,3] represent the most popular donor π-systems and have been extensively used in conducting and superconducting radical cation salts, as well as the donors obtained from the incorporation of Se and Te atoms in the TTF skeleton.[4,5]

The use of chalcogen atoms in the structure of the donor molecules has an important limitation involving a decrease in their solubility. Considering this limitation, non-planar molecules are expected to show higher solubility and their three-dimensional character may favor solid-state interactions. Working with this idea some different systems have been studied, including non-planar tetrathiafulvalene-functionalized systems with an increasing number of PPh_2 groups[6–11] (Fig. 1) and molecules with two or more redox centers (TTF) linked together in a non-planar arrangement.[12–16]

In this paper we report the reactivity of the tetrathiafulvalene-funcionalized phosphine tetrakis(diphenylphosphine)-tetrathiafulvalene, $(PPh_2)_4TTF$, (P4) with Cu(I), Ag(I) and Au(I) to give mono-, di- and tetra-nuclear derivatives. The solid-state characterization by X-ray analysis of one of these and of the P4 free ligand is also reported

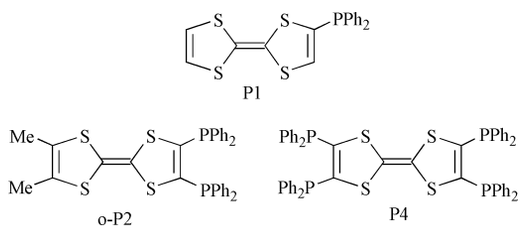

Fig. 1 Schematic representation of phosphine ligands based on tetrathiafulvalene.

Results and discussion

$(PPh_2)_4TTF$ (P4) was first prepared by Fourmigué *et al.*[6] by treatment of TTF with lithium diisopropylamide (LDA) and the subsequent addition of PPh_2Cl. Considering P4 as a tetradentate phosphine, we have performed different reactions in order to coordinate some different metallic centers, such as Cu(I), Ag(I) and Au(I).

The reaction of P4 (**1**) with gold(I) complexes with a labile ligand such as tht (tetrahydrothiophene) or $AsPh_3$ leads to the coordination of the metallic center to four phosphorus atoms of the P4 phosphines. Thus, starting with [AuX(tht)] (X = Cl, C_6F_5) or [Au(Mes)($AsPh_3$)] (Mes = 2,4,6-$Me_3C_6H_2$), complexes with the general formula $[(AuX)_4P4]$ (X = Cl, **2**; C_6F_5, **3**; Mes, **4**) (process i, Scheme 1) are obtained, by simple displacement of the labile ligand and posterior coordination of the metal to the P atom.

The IR spectra of complexes **2**–**4** do not show the characteristic bands of the tht or $AsPh_3$ ligands. Instead, we can identify

 DOI: 10.1039/b106310n

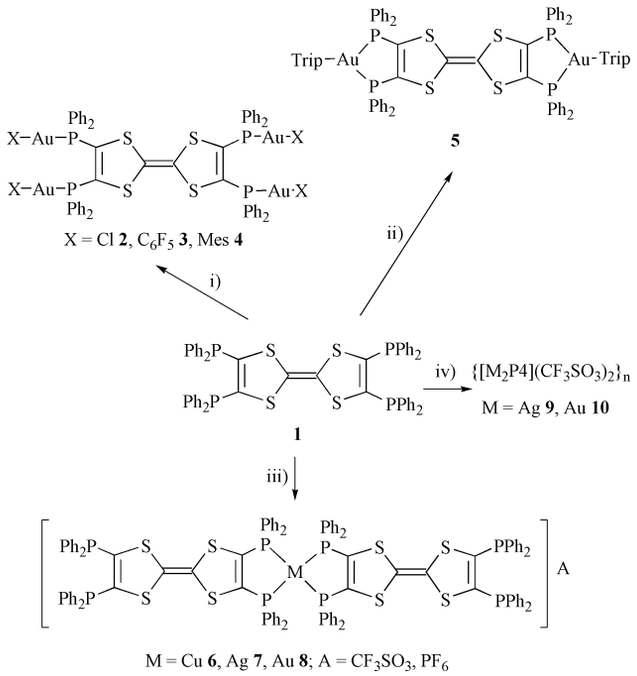

Scheme 1

vibrations due to the P4 ligand as well as ν(Au–Cl) at 355 cm^{-1} in the case of **2**, ν(Au–C_6F_5) at 956 and 793 cm^{-1} in **3** and the bands corresponding to the mesityl group[17] at 1655 and 843 cm^{-1} in complex **4**.

The ^{1}H NMR spectra show signals due to the phenyl groups as multiplets, and in the case of **4** the signals corresponding to the mesityl radical as singlets (protons from the *ortho*- and *para*-methyl groups and protons in the *meta* position). The $^{31}P\{^1H\}$ NMR spectra of complexes **2**–**4** display a singlet in all cases downfield displaced ($\Delta\delta$ = 40–50 ppm) compared with the value from the free ligand (−18.2 ppm).[6] The LSIMS+ mass spectra exhibit in complexes **2** and **3** the molecular peaks and additional peaks assignable to the fragmentation of the molecule. In the case of **4** only fragmentation peaks are present.

Molecular structure of $(PPh_2)_4TTF\cdot CHCl_3$ (1) and $[(AuCl)_4\{(PPh_2)_4TTF\}]\cdot CH_2Cl_2$ (2)

The crystalline structure of the dichloromethane solvate of complex **2** has been studied by X-ray analysis, in addition to the structure of the chloroform solvate of P4 (**1**) in order to compare the geometries. Drawings of both are depicted in Fig. 2

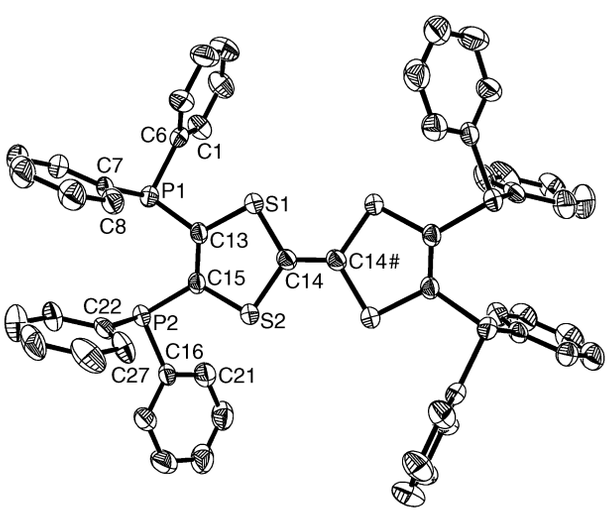

Fig. 2 Solid state structure of **1**. Displacement ellipsoids drawn at the 50% probability level. H atoms are omitted for clarity.

Table 1 Selected bond lengths (Å) and angles (°) for **1**

S(2)–C(14)	1.763(4)	P(1)–C(13)	1.832(4)
S(2)–C(15)	1.764(4)	P(2)–C(15)	1.819(4)
S(1)–C(13)	1.761(4)	C(14)–C(14#)	1.340(8)
S(1)–C(14)	1.763(4)		
C(14)–S(2)–C(15)	95.7(2)	C(14#)–C(14)–S(1)	122.8(5)
C(13)–S(1)–C(14)	95.4(2)	S(2)–C(14)–S(1)	114.2(2)
C(13)–C(15)–S(2)	116.8(3)	C(7)–P(1)–C(6)	102.5(2)
C(13)–C(15)–P(2)	120.7(3)	C(7)–P(1)–C(13)	102.1(2)
S(2)–C(15)–P(2)	122.4(3)	C(6)–P(1)–C(13)	100.6(2)
C(15)–C(13)–S(1)	117.6(3)	C(15)–P(2)–C(22)	102.9(2)
C(15)–C(13)–P(1)	123.1(3)	C(15)–P(2)–C(16)	101.7(2)
S(1)–C(13)–P(1)	119.3(3)	C(22)–P(2)–C(16)	104.0(2)
C(14#)–C(14)–S(2)	123.1(5)		

Symmetry transformations used to generate equivalent atoms: # $-x+1$, $-y+2$, $-z$.

Table 2 Selected bond lengths (Å) and angles (°) for **2**

Au(1)–P(1)	2.216(3)	S(2)–C(1)	1.752(8)
Au(1)–Cl(1)	2.278(3)	S(2)–C(2)	1.759(10)
Au(1)–Au(2)	3.0081(8)	P(1)–C(3)	1.825(9)
Au(2)–P(2)	2.233(2)	P(2)–C(2)	1.812(9)
Au(2)–Cl(2)	2.288(3)	C(1)–C(1)^i	1.310(19)
S(1)–C(3)	1.739(9)	C(2)–C(3)	1.358(12)
S(1)–C(1)	1.773(9)		
P(1)–Au(1)–Cl(1)	174.41(10)	C(2)–P(2)–Au(2)	119.1(3)
P(1)–Au(1)–Au(2)	80.97(6)	C(1)^i–C(1)–S(2)	124.4(9)
Cl(1)–Au(1)–Au(2)	104.35(8)	C(1)^i–C(1)–S(1)	122.5(9)
P(2)–Au(2)–Cl(2)	172.10(10)	S(2)–C(1)–S(1)	113.1(5)
P(2)–Au(2)–Au(1)	90.11(6)	C(3)–C(2)–S(2)	116.1(7)
Cl(2)–Au(2)–Au(1)	93.59(7)	C(3)–C(2)–P(2)	128.9(8)
C(3)–S(1)–C(1)	95.8(4)	S(2)–C(2)–P(2)	114.9(5)
C(1)–S(2)–C(2)	95.9(4)	C(2)–C(3)–S(1)	117.6(7)
C(3)–P(1)–Au(1)	114.5(3)	C(2)–C(3)–P(1)	125.4(7)
C(2)–P(2)–C(41)	102.6(5)	S(1)–C(3)–P(1)	116.9(5)

Symmetry transformations used to generate equivalent atoms: $-x+1$, $-y+2$, $-z$.

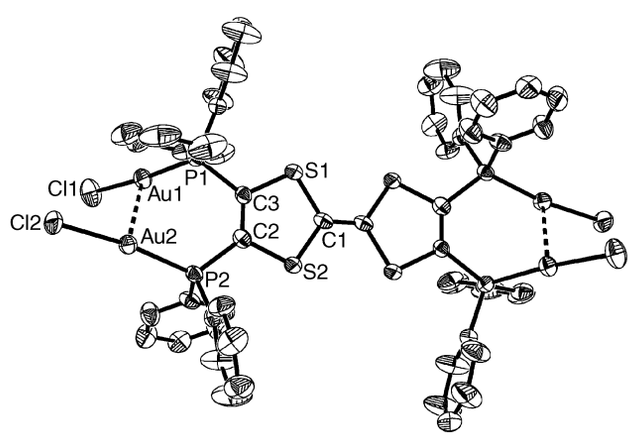

Fig. 3 Solid state structure of **2**. Displacement ellipsoids drawn at the 50% probability level. H atoms are omitted for clarity.

and 3. Selected bond distances and angles are provided in Tables 1 and 2.

P4 (**1**) lies about an inversion centre and there is also a 0.5 occupancy of chloroform of solvation disordered about another inversion centre. The $TTFP_4$ core is nearly planar with a dihedral angle between the planes (P1–C13–C15–P2) and (C13–S1–C14–S2–C15) of 1.1°. The representative distances C(14)–C(14#) = 1.340(8) Å, C(13)–C(15) = 1.353(6) Å and S(1/2)–C(14) = 1.763(4) Å, are essentially unchanged relative to

the bond lengths in TTF (1.35, 1.31 and 1.758 Å, respectively)[18] or in the bis-phosphine $TTF(Me)_2(PPh_2)_2$ [1.348(8), 1.344(6) and 1.753(5) Å, respectively].[6] The two phosphorus atoms adopt the usual distorted tetrahedral geometry with C–P–C angles being between 100.5 and 104.0°. The phosphorus–carbon TTF distances, P(1)–C(13) = 1.832(4) Å and P(2)–C(15) = 1.819(4) Å are similar to those reported for $TTF(Me)_2(PPh_2)_2$ [1.821(6) and 1.819(5) Å, respectively].[6] The molecules are packed with no short contacts between them (the shortest distance is *ca.* 8.076 Å). The arrangement of this packing produces channels as shown in Fig. 4, where the disordered chloroform of crystallization resides (omitted from the figure for clarity).

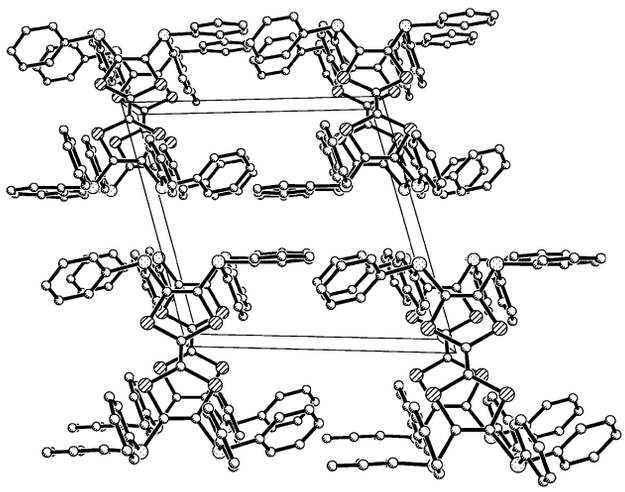

Fig. 4 Projection of the unit cell of **1** along [001].

Compound **2** crystallizes with a dichloromethane solvent molecule. The molecule again exhibits a crystallographic centre of symmetry and consists of one P4 unit with four Au–Cl units connected through the phosphorus atoms. In this case the TTFP4 core is slightly bent with a dihedral angle between the planes (P1–C3–C2–P2) and (C3–S1–C1–S2–C2) of 6°. The four Au–Cl units are above and below the TTFP4 plane. The coordination around the gold atoms deviates slightly from linearity, which is typical for gold(I) derivatives [P(1)–Au(1)–Cl(1) = 174.41(10)° and P(2)–Au(2)–Cl(2) = 172.10(10)°]. This is a consequence of the presence of an intramolecular interaction between the metallic centers Au(1) ··· Au(2) of 3.0081(8) Å, which is smaller than the sum of the van der Waals radii, illustrating the relativistic gold–gold contacts common for dinuclear gold(I) complexes.[19] The distances in the P4 core [C=C: 1.310(19), 1.358(12) Å and C–S: 1.773(9) and 1.752(8) Å] are similar to those found in the free phosphine. These data suggest that there a is non-important electronic change in the dithiole system due to the electronic donation of the phosphorus to the metal center. Apart from the intramolecular gold–gold interaction, there is an additional intermolecular contact of 3.402 Å between Au(1) and one chlorine atom from the CH_2Cl_2 solvent molecule, as is shown in Fig. 5. The packing of the molecules results in intermolecular distances of 7.303 Å (Fig. 5) between them. The Au–P [2.216(3), 2.233(2) Å] and Au–Cl [2.278(3), 2.288(3) Å] bond lengths are in the range of those found in dinuclear gold(I) derivatives with a bis-phosphine[20–23] as bidentate ligand.

When the same reaction described above is carried out with [Au(Trip)($AsPh_3$)] (process ii, Scheme 1), where Trip = 2,4,6-$Pr^i_3C_6H_2$ acts as a bulky radical, the results obtained, independently of the molar ratio used, give a dinuclear derivative with two Trip radicals instead of the homologous tetranuclear complexes **2**–**4**. Thus, [$(AuTrip)_2$P4] (**5**) can be isolated as an air-stable solid. As occurred in complexes **2**–**4** the $^{31}P\{^1H\}$ NMR spectra display a singlet due to the equivalence of the four

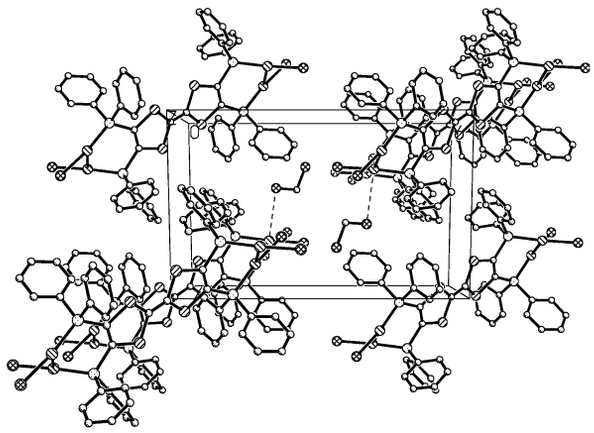

Fig. 5 Projection of the unit cell of **2** along [010].

P atoms. In ^1H NMR the signals from P4 and Trip keep a P4:Trip ratio of 1:2, which is in accordance with the proposed stoichiometry. In addition to these data, the mass spectrum displays the molecular peak, although with a small intensity [*m*/*z*(%) = 1741(5)], the corresponding fragmentation peak ($[M - Trip]^+$) and a higher *m*/*z* ratio, 1938 (6%), which can be identified as $[M + Au]^+$. The presence of the Trip radical, a high space-demanding group, can be the explanation for the isolation of the dinuclear compound instead of the tetranuclear one.

The P4 phosphine can also act as a bidentate ligand in the reaction with $[Cu(MeCN)_4]PF_6$, $AgCF_3SO_3$ or $[Au(tht)_2]$-CF_3SO_3 in a 2:1 molar ratio giving rise to $[M(P4)_2]A$ (A = PF_6, M = Cu, **6**; A = CF_3SO_3, M = Ag, **7**, Au, **8**) derivatives with two P4 units connected to the metallic center (process iv, Scheme 1).

The acetone solutions of complexes **6**–**8** show 1:1 electrolyte behavior[24] and the IR spectra display bands characteristic of an ionic PF_6 and triflate.[25]

The $^{31}P\{^1H\}$ NMR spectra of complexes **6**–**8** reveal two resonances: one for the coordinated phosphine groups, and one attributable to unbound phosphine at about −16 ppm. The former resonances are different in each derivative. Thus, the copper compound **6** displays a broad singlet at 4.8 ppm, even at low temperature; complex **7** displays a doublet of doublets as a consequence of the ^{107}Ag and ^{109}Ag nucleus coupling; and the gold derivative **8** shows one A_2B_2 spin system. The presence of such a system in the case of the gold complex indicates that the four phosphorus atoms are grouped in two pairs with a slight difference between them. This fact could be explained considering that the gold center is coordinated in a different way to the two pairs of P atoms. Unfortunately, we were not able to grow crystals suitable for X-ray analysis. In the case of the copper and silver derivatives we can imagine a tetrahedral geometry around the metallic centers, similar to those described in $[M(o\text{-}P2)_2]BF_4$ (M = Ag, Cu) complexes with o-P2 = 3,4-dimethyl-3′,4′-bis(diphenylphosphino)tetrathiafulvalene.[11]

The P4 ligand contains four binding sites in a *trans* position that can be used to join metals in oligomeric arrays. Working with this idea, we have investigated the reaction of P4 with gold(I) and silver(I) derivatives in a 1:1 molar ratio. Ratios of 1:2 or 1:4 have also been studied. In all the reactions only one stoichiometry is obtained, which can be represented by the general formula $\{[M_2P4](CF_3SO_3)_2\}_n$ (M = Ag, **9**; Au, **10**).

In the ^1H NMR spectra only signals corresponding to the PPh_2 groups are present in accordance with the proposed stoichiometry. The $^{31}P\{^1H\}$ NMR spectra display a doublet of doublets centered at −1.1 ppm in **9**, due to the presence of the ^{109}Ag and ^{107}Ag isotopomers and a singlet at 17.5 ppm in the gold compound. In the $^{19}F\{^1H\}$ NMR spectra appear one singlet in both cases centered at about −77.8 ppm, attributable to the presence of an anionic triflate.[26]

Table 3 Cyclic voltammetric data for P4 and related complexes (*V vs.* SCE, Pt disk electrode in 0.1 M of NBu_4PF_6)

Donor	$E^1_{1/2}$/V	$E_{(ox)}$/V	$E^2_{1/2}$/V
1; P4	0.33		0.73
2; $[(AuCl)_4P4]$	0.83		1.21
3; $[(AuC_6F_5)_4P4]$	0.76		1.16
4; $[(AuMes)_4P4]$	0.71	1.07	1.12
5; $[(AuTrip)_2P4]$	0.57		1.27
6; $[Cu(P4)_2](PF_6)$	0.61		0.81
7; $[Ag(P4)_2](CF_3SO_3)$	0.39	0.59	0.77
8; $[Au(P4)_2](CF_3SO_3)$	0.64		1.3
9; $\{[Ag_2P4](CF_3SO_3)_2\}_n$	0.82		1.11
10; $\{[Au_2P4](CF_3SO_3)_2\}_n$	0.79		1.08

The mass spectra (LSIMS+) show the molecular peak only in the case of the silver complex, in addition to lower peaks due to the fragmentation of the molecule and even higher peaks at *m*/*z*(%) = 1307 (12), 1989 (15) and 2247 (10) associated with $[M + CF_3SO_3]^+$, $[M + P4]^+$, $[M + P4 + CF_3SO_3]^+$, respectively. In complex **10** the highest peak, *m*/*z* = 1137, corresponds to the loss of one gold center.

Unfortunately, in the absence of single crystal X-ray data, we cannot draw any definitive conclusions about the nature of these complexes.

Visible-ultraviolet studies

The electronic absorbance spectra reveal, in all cases, the characteristic phenyl- and TTF-based transitions, which in the case of the free P4 phosphine appear at 212, 252, 320 and 432 nm. The extinction coeficients (ε) of these TTF bands are consistent with the number of chromophores in the molecule, when o-P2 is used as the TTF-functionalized phosphine.[7,9] We can extend these considerations to the case of $(PPh_2)_4TTF$. Thus, on the basis that P4, with four PPh_2 units (eight phenyl rings), shows a transition at 252 nm and has an ε of *ca.* 25000, complexes **2**–**5**, **9** and **10** show a slightly displaced transition from the value of 252 nm with similar ε values; however, complexes **6**–**8** display a double of the ε coefficient. With these data we assume the presence of only one P4 unit in complexes **2**–**5**, **9** and **10** and exactly double this number for complexes **6**–**8**.

Electrochemical studies

Cyclic voltammetry experiments display two, reversible one-electron oxidations to the mono- and di-cation species in all of the new complexes (Table 3). These oxidations occur at more positive potentials than the two reversible oxidations exhibited by the free P4 ligand,[6] except in the case of complex **7** where the values are similar to those found in the phosphine P4. This shift to higher potentials can be understood as a result of strong metal–P interactions. In the case of complexes **4** and **7** an additional oxidation process, without any reduction curve, is observed at $E_{(ox)}$ = 1.07 V (**4**) and 0.59 V (**7**), that can be assigned to a one-electron oxidation of the corresponding metal.

In conclusion, we have studied here the versatility of $(PPh_2)_4$-(TTF), whose structure has been presented, in the chemistry of group 11 metals. It can act as a bidentate or tetradentate ligand depending on the phosphine/metallic complex used, and regarding gold chemistry it affords two-, three- and four-coordinated gold(I) complexes. The two, reversible one-electron oxidations of $(PPh_2)_4$(TTF) are retained after the coordination, although they appear at higher potentials that in the free phosphine.

Experimental

General procedure

Starting materials: P4 (**1**),[6] [AuCl(tht)],[27] $[Au(C_6F_5)(tht)]$,[27] $[Au(Mes)(AsPh_3)]$[17] and $[Au(Trip)(AsPh_3)]$[28] were synthesised as previously reported. All other reagents were used as supplied. IR spectra were recorded on a Perkin Elmer 883 spectrophotometer, over the range 4000–200 cm^{-1}, using KBr pellets. ^1H, ^{31}P and ^{19}F NMR spectra were measured on a Varian UNITY 300 or BRUKER 300 spectrometer in $CDCl_3$ or $(CD_3)_2CO$ solution; chemical shifts are quoted relative to $SiMe_4$ (^1H), H_3PO_4 (external, ^{31}P) and $CFCl_3$ (external, ^{19}F). The C, H, N and S analyses were performed with a Perkin Elmer 2400 microanalyser. Mass spectra were recorded on a VG Autospec, by liquid secondary ion mass spectrometry (LSIMS+) using nitrobenzyl alcohol as matrix and a caesium gun. UV-vis spectra were recorded on a Unicam spectrometer in CH_2Cl_2 or MeCN solutions. Electrochemical measurements were recorded on a EG&G 273 model and carried out in dry CH_2Cl_2 or MeCN under argon using $[n\text{-}NBu_4]PF_6$ (0.1 M) as background electrolyte, with a Pt disk electrode *versus* SCE (values in V)

Syntheses

$[(AuX)_4P4]$ [X = Cl (2); C_6F_5 (3); Mes (4)]. To a solution of P4 (0.094 g, 0.1 mmol) in 10 ml of dichloromethane was added [AuCl(tht)] (0.128 g, 0.4 mmol), $[Au(C_6F_5)(tht)]$ (0.180 g, 0.4 mmol) or $[Au(Mes)(AsPh_3)]$ (0.248 g, 0.4 mmol). After 2 h of stirring, the solutions were concentrated and the addition of n-hexane led to the precipitation of pink (**2**,**3**) or red (**4**) solids, which were filtered off, washed with hexane and dried *in vacuo*. Yields: **2**, 83%; **3**, 78%; **4**, 55%.

2: Found: C, 34.29; H, 2.35; S, 6.68. $C_{54}H_{40}Cl_4P_4S_4Au_4$ requires: C, 34.67; H, 2.15; S, 6.85%. ^1H NMR ($CDCl_3$): δ 7.35–7.68 (m, Ph). $^{31}P\{^1H\}$ NMR ($CDCl_3$): δ 19.1 (s). UV-vis (CH_2Cl_2): λ_{max} (nm) (ε, M^{-1} cm^{-1}): 212 (7003), 252 (19588), 320 (13507), 432 (1591). CV (CH_2Cl_2): $E^1_{1/2}$ = 0.83 V, $E^2_{1/2}$ = 1.21 V. LSIMS+: *m*/*z* (%) 1868 (50, M^+), 1832 (100, $[M - Cl]^+$), 1597 (10, $[M - AuCl_2]^+$).

3: Found: C, 39.05; H, 1.82; S, 5.46. $C_{78}H_{40}F_{20}P_4S_4Au_4$ requires: C, 39.08; H, 1.68; S, 5.35%. ^1H NMR ($CDCl_3$): δ 7.33–7.66 (m, Ph). $^{31}P\{^1H\}$ NMR ($CDCl_3$): δ 21.3 (s). ^{19}F NMR: δ −117.1 (m, F_o), −161.21 (t, F_p), −165.5 (t, F_m). UV-vis (CH_2Cl_2): λ_{max} (nm) (ε, M^{-1} cm^{-1}): 212 (10699), 272 (27577), 325 (14712), 485 (668). CV (CH_2Cl_2): $E^1_{1/2}$ = 0.76 V, $E^2_{1/2}$ = 1.16 V. LSIMS+: *m*/*z* (%) 2395 (30, M^+), 2229 (15, $[M - C_6F_5]^+$), 2032 (20, $[M - AuC_6F_5]^+$), 1668 (12, $[M - 2AuC_6F_5]^+$).

4: Found: C, 49.47; H, 3.7; S, 6.15. $C_{90}H_{84}P_4S_4Au_4$ requires: C, 49.01; H, 3.35; S, 5.81%. ^1H NMR ($CDCl_3$): δ 7.33–7.63 (m, 40H, Ph), 6.59 (s, 8H), 2.17 (s, 12H, *p*-Me), 1.82 (s, 24H, *m*-Me). $^{31}P\{^1H\}$ NMR ($CDCl_3$): δ 30.9 (s). UV-vis (CH_2Cl_2): λ_{max} (nm) (ε, M^{-1} cm^{-1}): 212 (17164), 293 (39925), 480 (1865). CV (CH_2Cl_2): $E^1_{1/2}$ = 0.71 V, $E^2_{1/2}$ = 1.12 V. LSIMS+: *m*/*z* (%) 2085 (35, $[M - Mes]^+$), 1453 (55, $[M - 2Au - 3Mes]^+$), 1137 (20, $[P4 + Au]^+$).

$[(AuTrip)_2P4]$ (5). This was prepared as above starting from P4 (0.094 g, 0.1 mmol) and $[Au(Trip)(AsPh_3)]$ (0.140 g, 0.2 mmol). Yield: 70%. Found: C, 57.61; H, 4.82; S, 6.95. $C_{84}H_{86}P_4S_4Au_2$ requires: C, 57.92; H, 4.97; S, 7.36%. ^1H NMR ($CDCl_3$): δ 7.21–7.45 (m, 40H, Ph), 6.95 (s, 4H, *m*-H), 3.69 (sep, 4H, *o*-C*H*Me_2), 2.80 (sep, 2H, *p*-C*H*Me_2), 1.2 (d, 36H, *J* = 12 Hz, *p*-CH*Me*$_2$). $^{31}P\{^1H\}$ NMR ($CDCl_3$): δ 9.6 (s). UV-vis (CH_2Cl_2): λ_{max} (nm) (ε, M^{-1} cm^{-1}): 296 (35211), 347 (32042), 460 (2464). CV (CH_2Cl_2): $E^1_{1/2}$ = 0.57 V, E_{ox} = 1.07 V, $E^2_{1/2}$ = 1.27 V. LSIMS+: *m*/*z* (%) 1741 (5, M^+), 1537 (10, $[M - Trip]^+$), 1136 (6, $[P4 + Au]^+$), 1938 (6, $[M + Au]^+$).

$[M(P4)_2]A$ [M = Cu (6), A = PF_6; M = Ag (7), A = CF_3SO_3; M = Au (8), A = CF_3SO_3]. To a solution of P4 (0.188 g, 0.2 mmol) in 10 ml of dichloromethane under argon was added $[Cu(MeCN)_4](PF_6)$ (0.037 g, 0.1 mmol), $AgCF_3SO_3$ (0.025 g, 0.1 mmol) or $[Au(tht)_2](CF_3SO_3)$ (0.052 g, 0.1 mmol). After 3 h

Table 4 Summary of crystallographic data for derivatives P4·$CHCl_3$ (**1**) and $[(AuCl)_4P4]\cdot CH_2Cl_2$ (**2**)

Parameter	**1**	**2**
Empirical formula	$C_{55}H_{41}Cl_3P_4S_4$	$C_{56}H_{42}Au_4Cl_8P_4S_4$
M	1060.35	2038.48
T/K	150(2)	150(2)
Crystal system	Triclinic	Monoclinic
Space group	$P\bar{1}$	$P2_1/n$
a/Å	9.6800(9)	11.362(2)
b/Å	11.7691(10)	17.624(4)
c/Å	12.6621(12)	15.911(3)
α/°	72.829(6)	90
β/°	69.653(4)	104.99(3)
γ/°	82.261(5)	90
V/Å^3	1291.4(2)	3077.7(11)
Z	1	2
D_c/Mg m^{-3}	1.363	2.200
μ/mm^{-1}	0.500	10.129
Crystal size/mm	0.30 × 0.20 × 0.01	0.25 × 0.2 × 0.05
θ Range/°	2.94–23.26	2.96–25.03
$R1$ [a], $wR2$ [b] [$I > 2\sigma(I)$]	0.0587, 0.1614	0.0485, 0.1349
Max., min. residual density/e Å^{-3}	0.571, −0.558	2.110, −3.008

[a] $R1 = \Sigma||F_o| - \Sigma|F_c||/|F_o|$. [b] $wR2 = \{\Sigma[w(F_o^2 - F_c^2)]/\Sigma[w(F_o^2)^2]\}^{1/2}$.

of stirring, the solutions were concentrated and the addition of ethanol led to the precipitation of orange (**6**, **7**) and red (**8**) solids, which were filtered off, washed with ethanol and dried *in vacuo*. Yields: **6**, 70%; **7**, 60%; **8** 60%.

6: Found: C, 61.75; H, 3.86; S, 11.93. $C_{108}H_{80}P_9S_8F_6Cu$ requires: C, 62.05; H, 3.85; S, 12.26%. ^{1}H NMR (HDA): δ 7.15–7.49 (m, Ph). ^{31}P{^{1}H} NMR: δ 4.8 (s, br), −16.8 (s), −142.9 (sep). ^{19}F NMR: δ −70.6 (d, J_{P-F} = 702 Hz). UV-vis (CH_2Cl_2): λ_{max} (nm) (ε, M^{-1} cm^{-1}): 296 (52236), 327 (42163), 470 (8524). CV (CH_2Cl_2): $E^1_{1/2}$ = 0.61 V, $E^2_{1/2}$ = 0.81 V. LSIMS+: *m*/*z* (%) 1945 (6, M$^+$).

7: Found: C, 60.78; H, 4.05; S, 13.14. $C_{109}H_{80}O_3P_8S_9F_3Ag$ requires: C, 61.2; H, 3.77; S, 13.48%. ^{1}H NMR (HDA): δ 7.18–7.48 (m, Ph). ^{31}P{^{1}H} NMR (HDA, −85 °C): δ −1.3 (dd, $J_{^{107}Ag-P}$ = 235, $J_{^{109}Ag-P}$ = 270 Hz (s), −16.7 (s). ^{19}F NMR: δ −77.8 (s). UV-vis (CH_2Cl_2): λ_{max} (nm) (ε, M^{-1} cm^{-1}): 297 (45300), 321 (42779), 470 (3461). CV (CH_2Cl_2): $E^1_{1/2}$ = 0.39 V, E_{ox} = 0.59 V, $E^2_{1/2}$ = 0.77 V. LSIMS+: *m*/*z* (%) 1990 (5, M$^+$), 1050 (15, [P4 + Ag]$^+$).

8: Found: C, 58.41; H, 3.49; S, 13.10. $C_{109}H_{80}O_3P_8S_9F_3Au$ requires: C, 58.75; H, 3.61; S, 12.95%. ^{1}H NMR (HDA): δ 7.25–7.66 (m, Ph). ^{31}P{^{1}H} NMR (HDA): δ (A_2B_2) δ_A = 18.1, δ_B = 17.6, −16.8 (s). ^{19}F NMR: δ −77.8 (s). UV-vis (CH_2Cl_2): λ_{max} (nm) (ε, M^{-1} cm^{-1}): 268 (47491), 324 (25295), 463 (3846). CV (CH_2Cl_2): $E^1_{1/2}$ = 0.64 V, $E^2_{1/2}$ = 1.3 V. LSIMS+: *m*/*z* (%) 2078 (30, M$^+$), 1137 (15, [M − P4]$^+$), 940 (30, [P4]$^+$).

$\{[M_2P4](CF_3SO_3)_2\}_n$ [M = Ag (9); Au (10)]. To a solution of P4 (0.094 g, 0.1 mmol) in 10 ml of dichloromethane was added $[Au(tht)_2](CF_3SO_3)$ (0.104 g, 0.2 mmol) or $AgCF_3SO_3$ (0.051 g, 0.2 mmol). After 2 h of stirring, the solutions were concentrated and the addition of ethanol led to the precipitation of orange solids, which were filtered off, washed with ethanol and dried *in vacuo*. Yields: **9**, 75%: **10**, 50%.

9: Found: C, 46.5; H, 2.72; S, 13.6. $C_{56}H_{40}P_4S_6O_6F_6Ag_2$ requires: C, 46.23; H, 2.77; S, 13.22%. ^{1}H NMR (HDA): δ 7.18–7.48 (m, Ph). ^{31}P{^{1}H} NMR: δ −1.1 (dd, $J_{^{107}Ag-P}$ = 230, $J_{^{109}Ag-P}$ = 278 Hz (s). ^{19}F NMR: δ −77.7 (s). UV-vis (CH_2Cl_2): λ_{max} (nm) (ε, M^{-1} cm^{-1}): 262 (30842), 337 (19298), 450 (2631). CV (CH_2Cl_2): $E^1_{1/2}$ = 0.82 V, $E^2_{1/2}$ = 1.11 V. LSIMS+: *m*/*z* (%) 1154 (5, [M]$^+$), 1047 (55, [M − Ag]$^+$), 940 (55, [P4]$^+$), 1307 (15, [M + CF_3SO_3]$^+$), 1989 (15, [M + P_4 − Ag]$^+$), 2247 (10, [M + P_4 + CF_3SO_3]$^+$).

10: Found: C, 41.53; H, 2.82; S, 12.13. $C_{56}H_{40}P_4S_6O_6F_6Au_2$ requires: C, 41.19; H, 2.47; S, 11.78%. ^{1}H NMR (HDA): δ 7.27–7.50 (m, Ph). ^{31}P{^{1}H} NMR: δ 17.5 (s). ^{19}F NMR: δ −77.8 (s). UV-vis (MeCN): λ_{max} (nm) (ε, M^{-1} cm^{-1}): 281 (36377), 316 (30805). CV (MeCN): $E^1_{1/2}$ = 0.79 V, $E^2_{1/2}$ = 1.08 V. LSIMS+: *m*/*z* (%) 1137 (10, [M − Au]$^+$).

X-Ray studies

Single crystals of P4·$CHCl_3$ (**1**) and $[(AuCl)_4P4]\cdot CH_2Cl_2$ (**2**) were grown by slow diffusion of hexane into chloroform or dichloromethane solutions of their derivatives. Data collection at low temperature was carried out on a Bruker Nonius Kappa CCD diffractometer. Crystal parameters and experimental details are summarised in Table 4. The structures were solved by direct methods[29] and refined on F^2 by full-matrix, least squares using the program SHELXL-97.[30] Data were corrected for absorption using the SORTAV[31] program. All hydrogen atoms were located in geometric positions and refined using a riding model. In the case of **1** the $CHCl_3$ solvent molecule is disordered over two sites, each half occupied related by a centre; in **2** there is high thermal motion in the CH_2Cl_2 solvent molecule. Selected bond lengths and angles are given in Tables 1 and 2.

CCDC reference numbers 166713 and 166714.

See http://www.rsc.org/suppdata/dt/b1/b106310n/ for crystallographic data in CIF or other electronic format.

Acknowledgements

We thank the Spanish Directorate General for Higher Education and Scientific Research PB98–0542 for financial support. M. B. H. thanks the Engineering and Physical Sciences Research Council for support of the X-ray facilities.

References

1 R. E. Peierls, *Quantum Theory of Solids*, Oxford University Press, London, 1996.
2 M. Adam and K. Müllen, *Adv. Mater*, 1994, **6**, 439.
3 M. R. Bryce, *J. Mater. Chem.*, 1995, **5**, 1481.
4 J. A. Schlueter, U. Geiser, A. M. Kini, H. H. Wang, J. M. Williams, D. Naumann, T. Roy, B. Hoge and R. Eujen, *Coord. Chem. Rev.*, 1999, **192**, 781.
5 H. Kobayashi, A. Sato, H. Tanaka, A. Kobayashi and P. Cassoux, *Coord. Chem. Rev.*, 1999, **192**, 921.
6 M. Fourmigué, C. E. Uzelmeier, K. Boubekeur, S. L. Bartley and K. R. Dunbar, *J. Organomet. Chem.*, 1997, **529**, 343.
7 M. Fourmigué and P. Batail, *Bull. Soc. Chim. Fr.*, 1992, **129**, 29.
8 S. Jarchow, M. Fourmigué and Y.-S. Huang, *Acta Crystallogr., Sect. C*, 1993, **49**, 1936.
9 C. E. Ulzeimer, S. L. Bartley, M. Formigué, R. Rogers, G. Grandinetti and K. R. Dunbar, *Inorg. Chem*, 1998, **37**, 6706.
10 M. Asara, C. E. Ulzeimer, K. R. Dunbar and J. Alison, *Inorg. Chem.*, 1998, **37**, 1833.

11 B. W. Smucker and K. R. Dunbar, *J. Chem. Soc., Dalton Trans.*, 2000, 1309.
12 M. L. Kaplan, R. C. Haddon and F. Wudl, *J. Chem. Soc., Chem. Commun.*, 1977, 388.
13 K. Lerstrup, M. Jørgensen, I. Johannsen and K. Bechgaard, in *The Physics and Chemistry of Organic Superconductors*, G. Saito and S. Kagoshima, ed., Springer Verlag, Berlin, 1990, p. 383; K. Lerstrup and M. Jørgensen, *J. Org. Chem*, 1991, **56**, 5684.
14 M. Fourmigué and D. Batail, *J. Chem. Soc., Chem. Commun.*, 1991, 1370.
15 M. Fourmigué and Y.-H. Huang, *Organometallics*, 1993, **12**, 797.
16 F. Gerson, A. Lamprecht and M. Fourmigué, *J. Chem. Soc., Perkin Trans. 2*, 1996, 1409.
17 M. Contel, J. Jimenez, P. G. Jones, A. Laguna and M. Laguna, *J. Chem. Soc., Dalton Trans.*, 1994, 2515.
18 W. F. Cooper, J. W. Edmonds, F. Wudl and P. Coppens, *Cryst. Struct. Commun.*, 1974, **23**, 3; A. Ellern, J. Bernstein, J. Y. Becker, S. Zamir, L. Shaha and S. Cohen, *Chem. Mater.*, 1994, **6**, 1378.
19 P. Pyykkö, *Chem. Rev.*, 1997, **97**, 597.
20 H. Schmidbaur, W. Graf and G. Muller, *Angew. Chem., Int. Ed. Engl.*, 1988, **27**, 417.
21 D. S. Eggleston, D. F. Chodosh, G. R. Girard and D. T. Hill, *Inorg. Chim. Acta*, 1985, **108**, 221.
22 D. E. Eggleston, J. V. McArdle and G. E. Zuber, *J. Chem. Soc., Dalton Trans.*, 1987, 677.
23 H. Schmidbaur, C. Paschalidis, O. Steigelmann and G. Muller, *Chem. Ber*, 1989, **122**, 1851.
24 W. J. Geary, *Coord. Chem. Rev.*, 1971, **7**, 207.
25 D. H. Johnston and D. F. Shriver, *Inorg. Chem.*, 1993, **32**, 1045.
26 T. K. Hollis, N. P. Robinson and B. Bosnich, *Organometallics*, 1992, **11**, 2745.
27 R. Usón, A. Laguna and M. Laguna, *Inorg. Synth.*, 1989, **26**, 85.
28 E. Cerrada, M. Contel, A. D. Valencia, M. Laguna, T. Gelbrich and M. B. Hursthouse, *Angew. Chem., Int. Ed*, 2000, **39**, 2353.
29 G. M. Sheldrick, SHELXS-97: Fortran Program for Crystal Structure Solution, University of Göttingen, Germany, 1997.
30 G. M. Sheldrick, SHELXL-97: Fortran Program for Crystal Structure Refinement, University of Göttingen, Germany, 1997.
31 R. H. Blessing, *Acta Crystallogr., Sect. A*, 1995, **51**, 33; R. H. Blessing, *J. Appl. Crystallogr.*, 1997, **30**, 421.